Variational approach to bistable solitary waves of the first kind in d dimensions

R. H. Enns and S. S. Rangnekar
Department of Physics, Simon Fraser University, Burnaby, British Columbia, Canada V5A 1S6
(Received 21 May 1993)

The variational approach has been applied to a study of bistable solitary waves of the first kind in d dimensions for some illustrative models. In particular, energy formulas and bistability criterion have been derived and the variational results compared with those obtained numerically. In one dimension the agreement is found to be excellent. As d is increased, the agreement decreases despite the fact that flexibility was built into the trial wave function. The implications for successfully treating the three-dimensional light-bullet problem are discussed.

PACS number(s): 42.65.Pc, 42.50.Rh

I. INTRODUCTION

Bistable solitary-wave solutions to the one-dimensional generalized nonlinear Schrödinger equation (GNLSE) were described several years ago by Kaplan, Enns, and co-workers [1,2]. Since then the concept has been extended into higher spatial dimensions d, viz., the bistable "light bullet" for three dimensions [3–5]. For certain classes of intensity-dependent nonlinear refractive indices, it was shown that two or more solitary waves could exist with the same energy P but different propagation or phase-shift parameters δ. To distinguish this definition of bistability from one more recently introduced [6,7] into the literature we shall, following Ref. [8], refer to the associated solitary waves as bistable solitary waves of the first kind (BISOL1). The types of nonlinearity required for BISOL1 to occur for arbitrary d can be deduced as follows. For an intensity-(I) dependent nonlinearity of the form $f(I)=I^n$ with $n\geq 0$, it has been shown [3,5] that $dP/d\delta>0$ for $n<2/d$, $dP/d\delta=0$ for $n=2/d$, and $dP/d\delta<0$ for $n>2/d$. For $d=1$, 2, and 3, the critical (zero) slope value of n is 2, 1, and $\frac{2}{3}$, respectively. Thus BISOL1 are possible for $f(I)$ which are dominated by different n values in different ranges of I. Such behavior may occur in media for which different higher-order photon processes (an n-photon process yields an I^n contribution) dominate at different intensities. Alternately, one can [9] build up the requisite $f(I)$ by combining different media which are known to display saturable Kerr behavior. As simple *illustrative* examples of each possibility, consider the following nonlinearities.

(1) Polynominal model. $f(I)=a_1I+a_2I^3-a_3I^5$, with $a_1,a_2,a_3>0$.

(2) Saturable model.

$$f(I)=\frac{I}{f_{\rm sat}}\left[\frac{1}{(1+\bar{a}I)}+\frac{(1-\epsilon)}{(1+\bar{b}I)}-\frac{2(1-\epsilon)}{(1+\bar{c}I)}\right],$$

with $\bar{c}=\frac{1}{2}[\bar{a}/(1-\epsilon)+\bar{b}]$ and $f_{\rm sat}=\bar{a}^{-1}+(1-\epsilon)\bar{b}^{-1}-2(1-\epsilon)\bar{c}^{-1}$, with $\bar{a},\bar{b},\bar{c}>0$ and $0<\epsilon<1$.

Model 2 is similar to model 1 in that it is Kerr-like ($f\sim I$) at low I and rises like I^3 at intermediate I (due to the relation of $\bar{c}$ to $\bar{a},\bar{b}$). However, model 2 saturates to a constant value whereas in model 1, $f(I)$ eventually decreases with increasing I. This latter difference has implications as to stability, as we shall explain shortly.

For $d=1$, both models can yield N shaped $P(\delta)$ curves if the parameters are suitably adjusted. (For the polynomial model, the negative sign in the I^5 term changes the sign of the slope contribution.) *Numerically,* using the subscript cr to denote the critical value, one finds [2,9] that an N shape occurs for $R=a_1a_3/a_2^2<R_{\rm cr}\simeq 0.08$ for model 1 and, e.g., taking $\bar{a}=0.01$, $\bar{b}=0.05$, for $\epsilon<\epsilon_{\rm cr}\simeq 0.01-0.02$ for model 2. Models that yield N-shaped $P(\delta)$ curves in one dimension are particularly important because it is well known ([5] and references therein) that solitary waves corresponding to the positive-slope regions of the $P(\delta)$ curve are stable against weak perturbations while those corresponding to negative slope are absolutely unstable. Thus N-shaped $P(\delta)$ curves allow for two stable branches, which has been exploited by Enns at *et al.* [5] in their study of optical switching between "low" and "high" bistable soliton states. They have further shown [2] that for $f(I)$ which are Kerr-like at small I, rise like I^3 or faster at intermediate I, and either saturate or become Kerr-like again at large I, the solitary waves belonging to both the lower and upper positive-slope legs (low and high states) of the N-shaped energy curve are stable against *large* perturbations. The solitary waves are solitonlike. The saturable model 2 is an example of such an $f(I)$. For the polynomial model, the upper positive-slope solitary waves have been found [2] to be unstable against *sufficiently large* perturbations.

This stability issue aside, for most $f(I)$ (including models 1 and 2), one cannot *analytically* determine the *exact* solitary-wave shapes, the exact $P(\delta)$ relation, or, most importantly, the condition on the model parameters for bistability (i.e., the N shape) to occur. As in Refs. [2–5], one has resorted in general to numerical techniques, except for some artificially constructed (e.g., the "linear plus smooth step" model [2–5]) $f(I)$ which permitted exact analytic solutions. Following the variational approach of Desaix, Anderson, and Lisak [10], we shall show here, for the two illustrative models, that for $d=1$, the variational approach can yield *accurate analytic for-*

mulas for $P(\delta)$ and the bistability criterion. The corresponding trial wave functions are, of course, also accurate analytic representations of the solitary-wave shapes.

The variational approach is readily applicable to higher dimensions. For the two models considered here, the qualitative criterion mentioned earlier indicates that U-shaped $P(\delta)$ curves are possible for $d=2$ and 3. In this case, only one stable branch is possible, viz., the upper positive-slope leg of the U. Enns and co-workers [3–5] have created $f(I)$ which yield N- or W-shaped $P(\delta)$ curves in three dimensions, i.e., $f(I)$ which have *two stable branches.* The low and high state bistable light bullets of Refs. [3–5] correspond to these two branches. Before attempting to tackle these more complex $f(I)$, it is desirable to test the variational approach for $d=2$ and 3 on the simpler $f(I)$ characterized by models 1 and 2.

So in the next section we shall apply the variational method to both models for arbitrary d. In Sec. III we shall compare the variational results with those obtained numerically. In particular, we shall concentrate on the energy formulas and the bistability criterion. In Sec. IV we shall discuss the potential application of the variational method to the three-dimensional (3D) bistable light-bullet problem.

II. VARIATIONAL CALCULATION

In d dimensions, the intensity-dependent GNLSE takes the form (assuming anomalous dispersion and symmetric solutions)

$$i\frac{\partial u}{\partial \xi}+\frac{1}{2}\frac{1}{\rho^{d-1}}\frac{\partial}{\partial \rho}\left[\rho^{d-1}\frac{\partial u}{\partial \rho}\right]+f(I\equiv|u|^2)u=0\ , \tag{1}$$

where for the optical problem, u is proportional to the electric-field amplitude; ξ to the distance coordinate in the direction of propagation; $\rho=\sqrt{\xi^2+\eta^2+\tau^2}$ where ξ, η are normalized space coordinates in the transverse directions and τ is the normalized time, and $f(I)$ is proportional to the intensity-dependent part of the refractive index [1–5,10]. The Lagrangian associated with Eq. (1) is

$$L=\frac{i}{2}\left[u\frac{\partial u^*}{\partial \xi}-u^*\frac{\partial u}{\partial \xi}\right]\rho^{d-1}+\frac{1}{2}\left|\frac{\partial u}{\partial \rho}\right|^2\rho^{d-1}-F(|u|^2)\rho^{d-1}\ , \tag{2}$$

where

$$F(I)=\int_0^I f(I')dI'$$

and the asterisk denotes complex conjugate.

The form of the Lagrangian may be verified by noting that Eq. (1) results on substituting (2) into the variational equation [10,11]

$$\frac{\delta L}{\delta u^*}\equiv\frac{\partial}{\partial \xi}\left[\frac{\partial L}{\partial\left[\frac{\partial u^*}{\partial \xi}\right]}\right]+\frac{\partial}{\partial \rho}\left[\frac{\partial L}{\partial\left[\frac{\partial u^*}{\partial \rho}\right]}\right]-\frac{\partial L}{\partial u^*}=0\ . \tag{3}$$

As a trial wave function, we take

$$u(\rho,\xi)=A(\xi)\,\mathrm{sech}^m\left[\left[\frac{\rho}{a(\xi)}\right]^n\right]\exp[ib(\xi)\rho^2]\ , \tag{4}$$

with m,n positive real numbers. The amplitude A is allowed to be complex while the width $a(\xi)$ and "chirp" parameter $b(\xi)$ are real. By choosing different m and n we build some flexibility into our trial wave function. Of course, completely different forms (e.g., Gaussian) could also be chosen but the choice is severely limited by the necessity to be able to do the relevant integrals.

Substituting the assumed form (4) into Eq. (2), we next form the "reduced" Lagrangian, viz.,

$$\langle L\rangle=\int_0^\infty L d\rho=\frac{i}{2}\left[A\frac{dA^*}{d\xi}-A^*\frac{dA}{d\xi}\right]\frac{a^d}{n}I_{d/n-1,2m}+|A|^2\left[\frac{db}{d\xi}+2b^2\right]\frac{a^{d+2}}{n}I_{(d+2)/n-1,2m}+\frac{1}{2}|A|^2m^2na^{d-2}\gamma_{(d-2)/n+1,2m}-\frac{a^d}{n}\int_0^\infty F(|A|^2\mathrm{sech}^{2m}z)z^{d/n-1}dz\ , \tag{5}$$

with

$$I_{\alpha,\beta}=\int_0^\infty z^\alpha\mathrm{sech}^\beta z\,dz \tag{6a}$$

and

$$\gamma_{\alpha,\beta}=I_{\alpha,\beta}-I_{\alpha,\beta+2}\ . \tag{6b}$$

Some explicit values of $I_{\alpha,\beta}$ are given in Table I. These will be needed for the discussion in Secs. III and IV. Using the reduced Lagrangian (5), we then calculate

$$\frac{\delta\langle L\rangle}{\delta A^*}\equiv\frac{\partial}{\partial \xi}\left[\frac{\partial\langle L\rangle}{\partial(dA^*/d\xi)}\right]-\frac{\partial\langle L\rangle}{\partial A^*}=0\ ,$$
$$\frac{\delta\langle L\rangle}{\delta A}=0\ ,\quad \frac{\delta\langle L\rangle}{\delta a}=0\ ,\quad \frac{\delta\langle L\rangle}{\delta b}=0 \tag{7}$$

from which it follows, after straightforward algebra, that

$$|A|^2a^d=\mathrm{const}\equiv\mathcal{J}_0=(n/I_{d/n-1,2m})P\ , \tag{8}$$

TABLE I. $I_{\alpha,\beta}=\int_0^\infty z^\alpha \mathrm{sech}^\beta z dz$. G is Catalan's constant, which is equal to 0.915 965 594. n denotes numerically evaluated.

β \ α	0	1	2
1	$\pi/2$	$2G$	$\pi^3/8$
2	1	ln2	$\pi^2/12$
3	$\pi/4$	0.415 965 594 2^n	0.367 095 965 7^n
4	2/3	(4 ln2 − 1)/6	$\pi^2/18-1/3$
6	8/15	(8/15)ln2 − 11/60	0.105 315 751 2^n
8	16/35	(48 ln2 − 19)/105	0.064 873 818 45^n
10	128/315	(128/315)ln2 − 1321/7560	0.044 967 203 71^n
12	256/693	(256/693)ln2 − 6983/41580	0.033 491 108 71^n

with the energy

$$P=\int_0^\infty |u|^2\rho^{d-1}d\rho\ , \tag{9}$$

$$b=\frac{1}{2a}\frac{da}{d\xi}\ , \tag{10}$$

$$\frac{d^2a}{d\xi^2}-\frac{m^2n^2}{a^3}\left[\frac{\gamma_{(d-2)/n+1,2m}}{I_{(d+2)/n-1,2m}}\right]-\frac{d}{I_{(d+2)/n-1,2m}|A|^2a}\int_0^\infty [F(I)-If(I)]z^{d/n-1}dz=0\ , \tag{11}$$

$$\delta=\frac{i[A(dA^*/d\xi)-A^*(dA/d\xi)]}{2|A|^2}$$
$$=-\frac{m^2n^2}{a^2}\left[\frac{\gamma_{(d-2)/n+1,2m}}{I_{d/n-1,2m}}\right]+\frac{1}{I_{d/n-1,2m}|A|^2}\int_0^\infty\left[\left[1+\frac{d}{2}\right]If(I)-\frac{d}{2}F(I)\right]z^{d/n-1}dz\ , \tag{12}$$

with $I=|A|^2\mathrm{sech}^{2m}z$ in Eqs. (11) and (12).

To proceed any further we must insert specific forms of $f(I)$. We shall now consider the models introduced in the preceding section.

A. Polynomial model

Evaluating $F(I)$, we have

$$F(I)=\tfrac{1}{2}a_1I^2+\tfrac{1}{4}a_2I^4-\tfrac{1}{6}a_3I^6\ . \tag{13}$$

Equations (11) and (12) then become

$$\frac{d^2a}{d\xi^2}-\frac{m^2n^2}{a^3}\left[\frac{\gamma_{(d-2)/n+1,2m}}{I_{(d+2)/n-1,2m}}\right]+\frac{1}{2}\frac{a_1d\mathcal{I}_0}{a^{d+1}}\left[\frac{I_{d/n-1,4m}}{I_{(d+2)/n-1,2m}}\right]$$
$$+\frac{3}{4}\frac{a_2d\mathcal{I}_0^3}{a^{3d+1}}\left[\frac{I_{d/n-1,8m}}{I_{(d+2)/n-1,2m}}\right]-\frac{5}{6}\frac{a_3d\mathcal{I}_0^5}{a^{5d+1}}\left[\frac{I_{d/n-1,12m}}{I_{(d+2)/n-1,2m}}\right]=0\ , \tag{14}$$

which resembles an equation of motion, and

$$\delta=-\frac{m^2n^2}{a^2}\left[\frac{\gamma_{(d-2)/n+1,2m}}{I_{d/n-1,2m}}\right]$$
$$+a_1\left[1+\frac{d}{4}\right]|A|^2\left[\frac{I_{d/n-1,4m}}{I_{d/n-1,2m}}\right]$$
$$+a_2\left[1+\frac{3d}{8}\right]|A|^6\left[\frac{I_{d/n-1,8m}}{I_{d/n-1,2m}}\right]$$
$$-a_3\left[1+\frac{5d}{12}\right]|A|^{10}\left[\frac{I_{d/n-1,12m}}{I_{d/n-1,2m}}\right]\ . \tag{15}$$

Setting $y=a(\xi)/a_0$, where $a_0=a(0)$ is the initial width, and $dy/d\xi|_{\xi=0}=0$ (zero "initial velocity"), Eq. (14) can be integrated once to give the "energy" relation

$$\frac{1}{2}\left[\frac{dy}{d\xi}\right]^2+\mu\tilde{\pi}(y)=0\ , \tag{16}$$

with the "potential energy,"

$$\tilde{\pi}=\frac{\pi}{\mu}=\frac{1}{y^2}-\frac{B_1}{y^d}-\frac{B_2}{y^{3d}}+\frac{B_3}{y^{5d}}-(1-B_1-B_2-B_3)\ . \tag{17}$$

Here,

$$\mu=\frac{m^2n^2}{2a_0^4}\left[\frac{\gamma_{(d-2)/n+1,2m}}{I_{(d+2)/n-1,2m}}\right]$$

and, corresponding to the coefficients a_i, the B_i are given by

$$B_1=a_1\left[\frac{a_0^{2-d}\mathcal{J}_0}{m^2n^2}\right]\left[\frac{I_{d/n-1,4m}}{\gamma_{(d-2)/n+1,2m}}\right],$$
$$B_2=a_2\left[\frac{a_0^{2-3d}\mathcal{J}_0^3}{2m^2n^2}\right]\left[\frac{I_{d/n-1,8m}}{\gamma_{(d-2)/n+1,2m}}\right], \quad (18)$$
$$B_3=a_3\left[\frac{a_0^{2-5d}\mathcal{J}_0^5}{3m^2n^2}\right]\left[\frac{I_{d/n-1,12m}}{\gamma_{(d-2)/n+1,2m}}\right].$$

It should be noted that since the $B_i>0$, collapse of any input pulse to zero width ($y=0$) cannot occur because the B_3/y^{5d} term dominates. For the Kerr case ($B_2=B_3=0$) collapse can occur for $d=2$ and 3, as noted by Desaix, Anderson, and Lisak [10].

To obtain the parameters appropriate to the solitary-wave solution, we impose the stationary condition $d\bar{\pi}(y)/dy|_{y=1}=0$ which yields, on setting $|A(y=1)|=A_0$,

$$\frac{1}{a_0^2}=\frac{dA_0^2}{2m^2n^2\gamma_{(d-2)/n+1,2m}}\times\left[I_{d/n-1,4m}a_1+\frac{3}{2}I_{d/n-1,8m}A_0^4a_2-\frac{5}{3}I_{d/n-1,12m}A_0^8a_3\right]. \quad (19a)$$

Equation (19a) gives the necessary relation between the width a_0 and height A_0 for the solitary wave. Since $a=a_0$, then $b=0$ and $u(\rho,0)=A_0\mathrm{sech}^m[(\rho/a_0)^n]$ is the variational approximation to the solitary-wave shape.

Setting $A_0^2\equiv\sqrt{a_2/a_3}x^2$, $R\equiv a_1a_3/a_2^2$, and

$$Y(r\equiv\sqrt{a_1}(a_2/a_3)^{1/4}\rho)=(a_3/a_2)^{1/4}u(\rho,0),$$

the solitary-wave profile may be rewritten as $Y(r)=x\ \mathrm{sech}^m[(r/\bar{a}_0)^n]$ with

$$\frac{1}{\bar{a}_0}=\left[\frac{dI_{d/n-1,4m}}{2m^2n^2\gamma_{(d-2)/n+1,2m}}\right]^{1/2}\times x\left[1+\frac{3}{2}\left[\frac{I_{d/n-1,8m}}{I_{d/n-1,4m}}\right]\frac{x^4}{R}-\frac{5}{3}\left[\frac{I_{d/n-1,12m}}{I_{d/n-1,4m}}\right]\frac{x^8}{R}\right]^{1/2}. \quad (19b)$$

For given d, m, and n, specifying the normalized amplitude x determines the solitary-wave profile $Y(r)$ for each choice of R. Making use of Eqs. (15) and (19b), we calculate the normalized solitary-wave phase shift,

$$\beta\equiv\left[\frac{a_3}{a_2}\right]^{1/2}\frac{\delta}{a_1}=\left[1-\frac{d}{4}\right]\left[\frac{I_{d/n-1,4m}}{I_{d/n-1,2m}}\right]x^2+\left[1-\frac{3d}{8}\right]\left[\frac{I_{d/n-1,8m}}{I_{d/n-1,2m}}\right]\frac{1}{R}x^6-\left[1-\frac{5d}{12}\right]\left[\frac{I_{d/n-1,12m}}{I_{d/n-1,2m}}\right]\frac{1}{R}x^{10} \quad (20)$$

and normalized solitary-wave energy,

$$\bar{P}\equiv a_1^{d/2}\left[\frac{a_2}{a_3}\right]^{d/4-1/2}P=m^dn^{d-1}I_{d/n-1,2m}\left[\frac{2\gamma_{(d-2)/n+1,2m}}{dI_{d/n-1,4m}}\right]^{d/2}\frac{x^{2-d}}{\left[1+\frac{3}{2}\left[\frac{I_{d/n-1,8m}}{I_{d/n-1,4m}}\right]\frac{1}{R}x^4-\frac{5}{3}\left[\frac{I_{d/n-1,12m}}{I_{d/n-1,4m}}\right]\frac{1}{R}x^8\right]^{d/2}}. \quad (21)$$

By specifying x (i.e., A_0) one may calculate β from (20), $\bar{P}$ from (21), and then plot $\bar{P}$ vs β.

B. Saturable model

$$F(I)=I-[\bar{a}^{-2}\ln(1+\bar{a}I)+(1-\epsilon)\bar{b}^{-2}\ln(1+\bar{b}I)-2(1-\epsilon)\bar{c}^{-2}\ln(1+\bar{c}I)]/f_{\mathrm{sat}}. \quad (22)$$

Unlike the situation for the polynominal model, the integrals in Eqs. (11) and (12) cannot be carried out for general m,n. One case which can be solved is $m=\frac{1}{2}$, $n=d$ for which the potential energy is given by

$$\bar{\pi}=\frac{\pi(y)}{\bar{\mu}}=\frac{1}{y^2}-1+\theta[H_{\bar{A}}(y)+(1-\epsilon)H_{\bar{B}}(y)-2(1-\epsilon)H_{\bar{C}}(y)], \quad (23)$$

where

$$H_X(y)\equiv\left\{\frac{\pi^2}{4d^2}(y^d-1)+(\arccos X)^2-y^d\left[\arccos\left[\frac{X}{y^d}\right]\right]^2\right\}\Big/X^2, \quad (24)$$

$$\bar{\mu}\equiv d^2\gamma_{2-2/d,1}/8a_0^4 I_{2/d,1},$$
$$\theta\equiv 4a_0^2 A_0^2/f_{\rm sat}\gamma_{2-2/d,1}\ , \tag{25}$$

and $\bar{A}=\bar{a}A_0^2$, $\bar{B}=\bar{b}A_0^2$, $\bar{C}=\bar{c}A_0^2$.

Also

$$\frac{1}{a_0^2}=\frac{2A_0^2}{d\gamma_{2-2/d,1}f_{\rm sat}} \times[h(\bar{A})+(1-\epsilon)h(\bar{B})-2(1-\epsilon)h(\bar{C})]\ , \tag{26}$$

with

$$h(X)=\left[\frac{\pi^2}{4}-(\arccos X)^2-2\frac{X\arccos X}{\sqrt{1-X^2}}\right]\Big/X^2\ , \tag{27}$$

$$\bar{P}\equiv\frac{(\bar{a}d)^{1-d/2}2^{1+d/2}P}{\pi(\gamma_{2-2/d,1}f_{\rm sat})^{d/2}} =\frac{\bar{A}^{1-d/2}}{[h(\bar{A})+(1-\epsilon)h(\bar{B})-2(1-\epsilon)h(\bar{C})]^{d/2}}\ , \tag{28}$$

and

$$\delta=1-\left[\frac{d}{2\pi}\right]\frac{[g(\bar{A})+(1-\epsilon)g(\bar{B})-2(1-\epsilon)g(\bar{C})]}{[\bar{A}^{-1}+(1-\epsilon)\bar{B}^{-1}-2(1-\epsilon)\bar{C}^{-1}]}\ , \tag{29}$$

where

$$g(X)=\frac{4}{d}\frac{\arccos X}{X\sqrt{1-X^2}}+h(X)\ . \tag{30}$$

Note that in using the analytic forms (26)–(30), one is limited by the fact that the arguments of the arccos terms cannot exceed unity. When any one of the arguments increases above one, no simple analytic form for the relevant integrals exists.

III. COMPARISON OF VARIATIONAL AND NUMERICAL RESULTS

Since the emphasis in this paper is on the bistability aspects, we would like to compare the variational energy formulas with numerically obtained results. Taking the polynomial model as an example, the numerical $\bar{P}(\beta)$ curve is obtained as follows. Assuming that $u(\rho,\zeta)=V(\rho)e^{i\delta\zeta}$ and setting $Y=(a_3/a_2)^{1/4}V$, $r=a_1^{1/2}(a_2/a_3)^{1/4}\rho$, Eq. (1) yields

$$\frac{rd^2Y}{dr^2}+\frac{(d-1)dY}{dr} +2r\left[-\beta Y+Y^3+\frac{1}{R}Y^7-\frac{1}{R}Y^{11}\right]=0\ . \tag{31}$$

To obtain a solitary-wave solution, we want $Y=Y_{\max}$, $dY/dr=0$ at $r=0$, and both Y and $dY/dr\to 0$ as $r\to\infty$. For given β and R, Eq. (31) is numerically integrated for different $Y_{\max}$ until an amplitude is found for which the asymptotic ($r\to\infty$) boundary conditions are satisfied. With the solitary-wave profile $Y_{\rm sol}(r)$ then known, the normalized energy is then calculated numerically from

$$\bar{P}=\int_0^\infty Y_{\rm sol}^2(r)r^{d-1}dr\ . \tag{32}$$

To be consistent with standard practice in earlier papers [1,2], for 1D the numerical energy result is multiplied by 2 since the limits really should be from $-\infty$ to $+\infty$. We first look at the 1D results, then at higher dimensions.

A. One-dimensional results

We start with the polynomial model. In the Kerr limit ($a_2=a_3=0$), the choice $m=n=1$ yields the *exact* analytic solitary-wave solution. In terms of $R=a_1a_3/a_2^2$, this limit corresponds to $R\to\infty$. Thus for large R we might anticipate that for the complete polynomial the trial wave function with $m=n=1$ might be a reasonably good approximation to the exact (numerical) solitary-wave profile. But, as already mentioned in the Introduction, we known from previous numerical studies that for bistability (i.e., an N-shaped energy curve) to occur we must have $R<R_{\rm cr}\simeq 0.08$. How good is the $m=n=1$ variational result for such low R values? Would we be better off to make other choices for m and n? From Eqs. (20) and (21) and Table I, we obtain for $m=n=1$ the following formulas for the phase shift and energy:

$$\beta_{\rm var}=\left[\frac{1}{2}\right]x^2+\left[\frac{2}{7R}\right]x^6-\left[\frac{64}{297R}\right]x^{10}\ , \tag{33}$$

$$\bar{P}_{\rm var}=\frac{x}{[1+(36/35R)x^4-(640/693R)x^8]^{1/2}}\ . \tag{34}$$

In Fig. 1 we have plotted $\bar{P}_{\rm var}(\beta_{\rm var})$ given by (33), (34) as well as the numerical $\bar{P}(\beta)$ for $R=0.01<R_{\rm cr}$. The agreement is remarkably good. A minor discrepancy occurs, however, high on the upper positive-slope leg of the N. This is better seen in the inset where we have magnified the relevant region and used a linear scale for β rather than the log scale of the main figure. Numerically

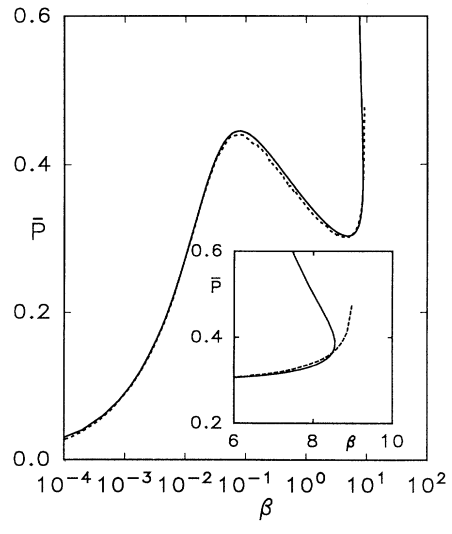

FIG. 1. One-dimensional $\bar{P}(\beta)$ curve for the polynomial model with $R=0.01$. Numerical, dotted curve; $m=n=1$ [Eqs. (33), (34)] variational formula, solid curve. Inset: enlarged view of upper end of $\bar{P}(\beta)$ curve.

$d\bar{P}/d\beta$ remains positive whereas the variational curve has a negative slope. The latter implies absolute instability, whereas it has been previously observed [2] through collision studies that the high state solitary waves are stable against small perturbations. The source of the discrepancy lies in the behavior of the phase-shift formula (33) at sufficiently large x. That this is so follows from the fact that in 1D (but not for higher d), β may be derived *exactly*. Equation (31) can be integrated once to yield

$$\frac{1}{2}\left[\frac{dY}{dr}\right]^2=\beta Y^2-\frac{1}{2}Y^4-\frac{1}{4R}Y^8+\frac{1}{6R}Y^{12}\ . \tag{35}$$

Then, setting $Y=Y_{\max}=x=(a_3/a_2)^{1/4}A_0$ and $dY/dr=0$ in Eq. (35), we obtain

$$\beta_{\text{exact}}=\left[\frac{1}{2}\right]x^2+\left[\frac{1}{4R}\right]x^6-\left[\frac{1}{6R}\right]x^{10}\ . \tag{36}$$

For $R\to\infty$, $\beta_{\text{var}}=\beta_{\text{exact}}=\beta_{\text{Kerr}}=\frac{1}{2}x^2$, the *exact* Kerr phase-shift formula. The Kerr phase shift increases continuously with x, but for the polynomial model, β eventually decreases at large enough x. In Fig. 2, we have plotted Eqs. (33) and (36) for two different R values, $R=0.1$ and 0.01. The agreement between the two curves is better over a wider range of x for the larger R value. In either case the variational β curve peaks slightly earlier as a function of x than the exact result. For $R=0.01$, the R value of Fig. 1, one finds that $\bar{P}_{\text{num}}(\simeq\bar{P}_{\text{exact}})\to\infty$ as β_{exact} approaches its maximum value. The β_{var} curve decreases prematurely, leading to the spurious negative slope in $\bar{P}_{\text{var}}$ at large β. That the variational phase-shift formula is less accurate than the variational energy formula follows by plotting (not shown here) $\bar{P}$ vs β_{exact}. The agreement with the numerical energy curve in Fig. 1 is essentially perfect. However, referring to Fig. 1 again, let us emphasize that $\bar{P}_{\text{var}}$ vs β_{var} gives a very good fit to the numerical energy curve, other choices of m and n being less accurate.

For example, for $m=\frac{1}{2}$, $n=1$, one obtains from Eqs. (20), (21), and Table I,

$$\beta=\left[\frac{3}{\pi}\right]\left[\left[\frac{1}{2}\right]x^2+\left[\frac{5}{18R}\right]x^6-\left[\frac{28}{135R}\right]x^{10}\right]\ , \tag{37}$$

$$\bar{P}=\frac{(\pi/4)\sqrt{\pi/2}x}{[1+(1/R)x^4-(8/9R)x^8]^{1/2}}\ , \tag{38}$$

which is plotted in Fig. 3 for $R=0.01$ and compared to the numerical curve. For $m=\frac{1}{2}$, $n=1$, β_{var} only reaches 8.07 compared to $\beta_{\text{var}}\simeq 8.56$ for $m=n=1$. Furthermore, β differs from β_{exact} as $R\to\infty$ by the factor $3/\pi\simeq 0.955$.

As a corollary to this, one might expect to calculate R_{cr} fairly accurately from the variational formulas for $m=n=1$. When an N-shaped energy curve is present, $d\bar{P}_{\text{var}}/d\beta_{\text{var}}$ has two zeros corresponding to a maximum (upper end of the lower positive-slope leg) and a minimum (lower end of the upper positive-slope leg). As R is increased, the two zeros move towards each other and coalesce when R_{cr} is reached. For $R>R_{\text{cr}}$, there is no real zero and bistability vanishes.

From Eqs. (33) and (34) on forming

$$\frac{d\bar{P}_{\text{var}}}{d\beta_{\text{var}}}=\left[\frac{d\bar{P}_{\text{var}}}{dx}\right]\Big/\left[\frac{d\beta_{\text{var}}}{dx}\right]=0\ ,$$

we obtain the location of the two zeros at

$$x_0=[(A\pm\sqrt{A^2-12B})/6B]^{1/4}\ , \tag{39}$$

with $A\equiv 36/35R$, $B\equiv 640/693R$. Coalescence occurs when $A^2=12B$, i.e., at $R_{\text{cr}}^{\text{var}}=2673/28\,000\simeq 0.095$. This is in good agreement with the numerically obtained value $R_{\text{cr}}^{\text{num}}=0.088$.

Turning now to the saturable model, we consider the same choices of $\bar{a},\bar{b},\epsilon$ as in Ref. [9] where $\bar{P}(\beta)$ was calculated numerically. For example, an N-shaped energy curve was observed for $\bar{a}=0.01$, $\bar{b}=0.04$, and $\epsilon=0.01$ as shown in Fig. 4. Also shown is the variational result calculated from Eqs. (28) and (29). The agreement between the two curves is excellent. The variational curve terminates at a finite β value because $\bar{B}=\bar{b}A_0^2$ reaches unity and the analytic forms (28) and (29) can no longer be used. Unfortunately, for larger β analytic forms do not exist for the relevant integrals.

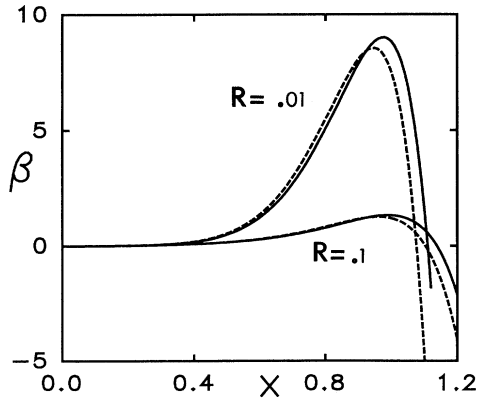

FIG. 2. Normalized phase-shift (β) dependence on normalized amplitude (x) for polynomial model in 1D with $R=0.1$ and 0.01. β_{exact} [Eq. (36)], solid curves; $m=n=1$ formula (Eq. (33) for β_{var}, dashed curves.

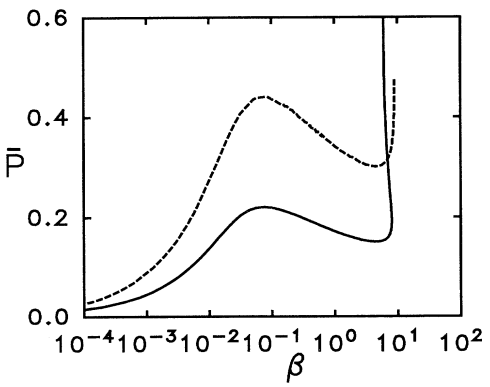

FIG. 3. 1D $\bar{P}(\beta)$ curve for polynomial model with $R=0.01$. Numerical, dashed curve; $m=\frac{1}{2}$, $n=1$ [Eqs. (37), (38)] variational result, solid curve.

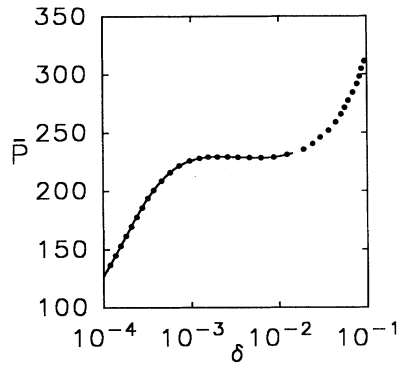

FIG. 4. 1D $\bar{P}(\delta)$ curve for saturable model with $\bar{a}=0.01$, $\bar{b}=0.04$, and $\epsilon=0.01$. Numerical, dotted curve; variational formula [Eqs. (28), (29) with $d=1$], solid curve.

As for the polynomial model, we can set $d\bar{P}/d\delta=(d\bar{P}/dA_0)/(d\delta/dA_0)=0$ and, say, for fixed $\bar{a},\bar{b},\bar{c}$ look for the critical value of ϵ,ϵ_{cr}, at which coalescence of the two zeros takes place. The result of this calculation is the transcendental equation

$$K(\bar{A})+(1-\epsilon)K(\bar{B})-2(1-\epsilon)K(\bar{C})=0\ , \tag{40}$$

with

$$K(X)=\left[\left[3\pi^2/4\right]-3(\arccos X)^2-\frac{2X^2}{(1-X^2)}+\frac{X(8X^2-6)\arccos X}{(1-X^2)^{3/2}}\right]\Big/X^2\ . \tag{41}$$

In Ref. [9] we found, e.g., for $\bar{a}=0.01$, $\bar{b}=0.05$, that $\epsilon_{cr}\simeq 0.01$–0.02. For $\epsilon>\epsilon_{cr}$, the N shape disappears and there is no bistability. For these $\bar{a},\bar{b}$ values one finds from Eqs. (40) and (41) that $\epsilon_{cr}=0.0140$, agreeing with the numerically observed value. Alternately, holding $\epsilon=0.01$, $\bar{a}=0.01$, and varying $\bar{b}$, we find from Eqs. (40) and (41) that $0.4<\bar{b}\lesssim 4$ for bistability to occur, in complete agreement with the numerical results obtained in Ref. [9].

Thus, at least for the two representative models considered here, the variational approach does an excellent job in 1D of accurately predicting the critical parameters for bistability to occur as well as the detailed shapes of the bistable energy curves. What is the situation for higher dimensions?

B. Two- and three-dimensional results

Again we look at the polynomial model first. Three different choices of m,n are considered for $d=2$, viz., making use of Table I, as follows.

(*i*) $m=n=1$.

$$\beta=\left[\frac{1}{3}-\frac{1}{12\ln 2}\right]x^2+\left[\frac{4}{35}-\frac{19}{420\ln 2}\right]x^6\Big/R-\left[\frac{128}{2079}-\frac{6983}{249\,480\ln 2}\right]x^{10}\Big/R\ , \tag{42}$$

$$\bar{P}=\frac{[(2\ln 2+1)\ln 2/(4\ln 2-1)]}{1+\left[\frac{3(48\ln 2-19)}{35(4\ln 2-1)}\right]\frac{x^4}{R}-\left[\frac{10(256\ln 2/693-6983/41\,580)}{(4\ln 2-1)}\right]\frac{x^8}{R}}\ . \tag{43}$$

(*ii*) $m=\frac{1}{2}$, $n=1$.

$$\beta=\left[\frac{\ln 2}{4G}\right]x^2+\left[\frac{(4\ln 2-1)}{48G}\right]x^6\Big/R-\left[\frac{(32\ln 2-11)}{720G}\right]x^{10}\Big/R\ , \tag{44}$$

$$\bar{P}=\frac{[G(2G-I_{1,3})/2\ln 2]}{1+[1-(1/4\ln 2)](x^4/R)-[8/9-(11/36\ln 2)]\frac{x^8}{R}}\ , \tag{45}$$

where G is Catalan's constant and the numerical value of $I_{1,3}$ is given in Table I.

(*iii*) $m=1,n=2$.

$$\beta=\left[\frac{1}{3}\right]x^2+\left[\frac{4}{35R}\right]x^6-\left[\frac{128}{2079R}\right]x^{10}\ , \tag{46}$$

$$\bar{P}=\frac{[(\ln 2+1/2)(\pi/4)]}{1+[36/35](x^4/R)-[640/693]\frac{x^8}{R}}\ . \tag{47}$$

Independent of the particular choice of m,n, the energy formula is of the general structure $\bar{P}\sim 1/[1+Ax^4+Bx^8]$, so that one finds zero slope occurring at $x_0=0$ (i.e., $\beta=0$) and $x_1=(A/2B)^{1/2}$. But the ratio A/B is independent of R so there is no R_{cr} for 2D. This conclusion is supported numerically and is consistent with the slope rules discussed in the Introduction, i.e., for any value of R, $\bar{P}$ starts out with zero slope, dips to a minimum at x_1 (i.e., at β_1), and then increases.

As to accuracy of fit, in Fig. 5 we have compared the three choices embodied in Eqs. (42)–(47) against the numerical energy curves for $R=0.1$ and 1. At low β, the first two choices fit well but deviate as β increases. As in 1D the $m=\frac{1}{2}$, $n=1$ curve turns upward before the $m=n=1$ curve. Reasoning that holding m at 1 but allowing n to increase would cause the energy curve to turn up later as a function of β, we considered $m=1$, $n=2$.

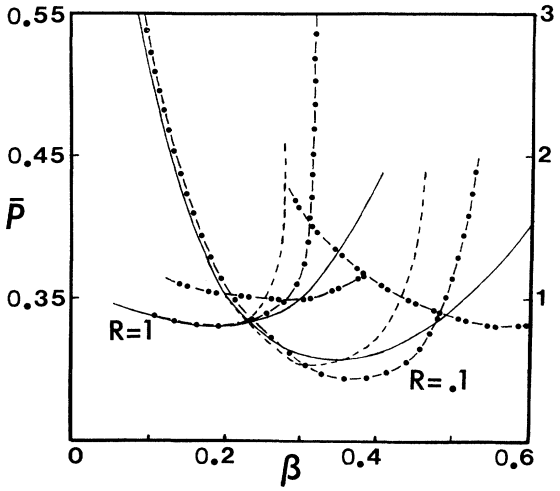

FIG. 5. 2D $\bar{P}(\beta)$ curve for polynomial model with $R=1$ (right ordinate) and $R=0.1$ (left ordinate). Numerical, solid curves; $m=n=1$ [Eqs. (42), (43)] formula, dash-dot curves; $m=\frac{1}{2}$, $n=1$ [Eqs. (44), (45)] formula, dashed curves; $m=1$, $n=2$ [Eqs. (46), (47)] formula, dash-plus-two-dot curves.

Indeed the energy curve does turn up later but the overall fit is very poor for both R values.

In Fig. 6, we have $d=3$ and again take $R=0.1$ and 1, U shapes occurring for any R. We consider the two following cases.

(*i*) $m=n=1$.

$$\beta=\left[\frac{1}{6}-\frac{1}{\pi^2}\right]x^2-\left[\frac{3I_{2,8}}{2\pi^2}\right]x^6/R + \left[\frac{3I_{2,12}}{\pi^2}\right]x^{10}/R \ , \tag{48}$$

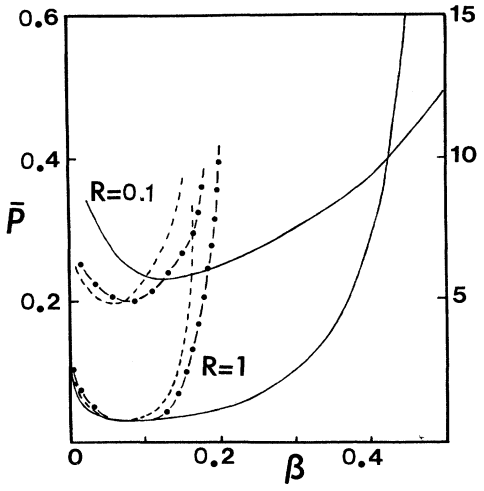

FIG. 6. 3D $\bar{P}(\beta)$ curve for polynomial model with $R=1$ (right ordinate) and 0.1 (left ordinate). Numerical, solid curves; $m=n=1$ [Eqs. (48), (49)] formula, dash-dot curves; $m=\frac{1}{2}$, $n=1$ [Eqs. (50), (51)] formula, dashed curves.

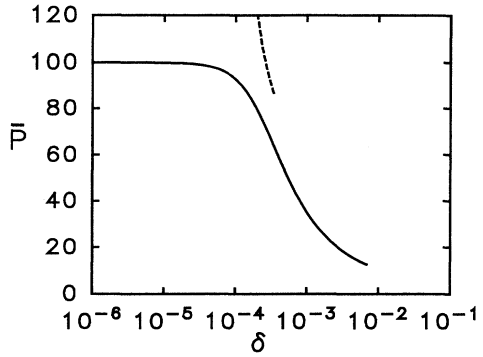

FIG. 7. Two- and three-dimensional variational $\bar{P}(\delta)$ curves for saturable model with $\bar{a}=0.01$, $\bar{b}=0.04$, and $\epsilon=0.01$. 2D, solid curve; 3D, dashed curve.

$$\bar{P}=\frac{(\pi^2/12)[(\pi^2+12)/(3\pi^2-18)]^{3/2}}{x\left[1+\left[\frac{27I_{2,8}}{(\pi^2-6)}\right]\frac{x^4}{R}-\left[\frac{30I_{2,12}}{(\pi^2-6)}\right]\frac{x^8}{R}\right]^{3/2}} \ , \tag{49}$$

where the numerically evaluated values of $I_{2,8}$ and $I_{2,12}$ are given in Table I.

(*ii*) $m=\frac{1}{2}$, $n=1$.

$$\beta=\left[\frac{1}{6\pi}\right]x^2-\left[\frac{(\pi^2-6)}{18\pi^3}\right]x^6/R+\left[\frac{2I_{2,6}}{\pi^3}\right]x^{10}/R \ , \tag{50}$$

$$\bar{P}=\frac{[(\pi^3/4)-2I_{2,3}]^{3/2}/8}{x\{1+[1-(6/\pi^2)]x^4/R-(20I_{2,6}/\pi^2)x^8/R\}^{3/2}} \ , \tag{51}$$

where $I_{2,3}$ and $I_{2,6}$ have been evaluated numerically. As one progresses from 1D to 3D, we see from Figs. 1, 5, and 6 that our trial wave functions progressively are less successful at producing good fits to the numerical energy curves. We have tried to include flexibility by allowing m and n to take on different values but in higher dimensions this is clearly not sufficient.

Finally, in Fig. 7 we show the two- and three-dimensional variational results for the saturable model with, e.g., $\bar{a}=0.01$, $\bar{b}=0.04$, and $\epsilon=0.01$. As expected from the guidelines in the Introduction, the 2D curve starts out with zero slope at very small δ. Both curves terminate at an upper limit of δ without revealing the positive-slope branch of the U-shaped energy curve which is observed numerically (not shown). Unlike the situation in 1D, the agreement with the numerical curves over most of the range shown in Fig. 7 was found to be quite poor.

IV. DISCUSSION

Although the variational method works extremely well in 1D in discussing BISOL1 for the representative models, in higher dimensions the method becomes less accurate, the variational energy curves deviating substantially from the numerical curves at larger β values for the polynomial model and prematurely terminating at some β

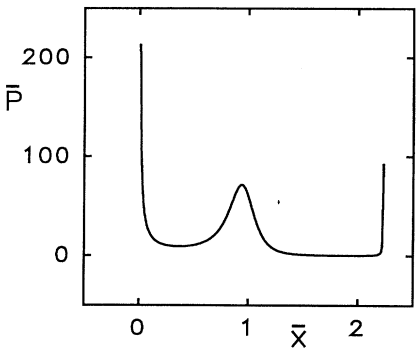

FIG. 8. Three-dimensional $\bar{P}(\bar{x})$ curve given by variational formula (53) for $\bar{R}=0.3$, $\bar{R}'=0.2$.

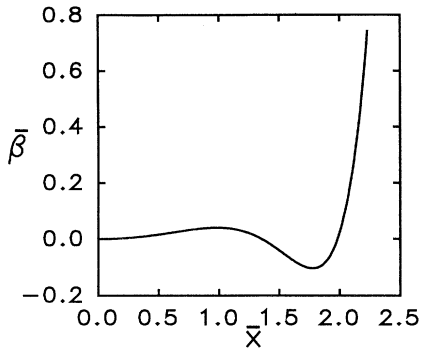

FIG. 9. Phase-shift formula (52) for $\bar{R}=0.3$, $\bar{R}'=0.2$.

value for the saturable model. Of course this is an indication that our trial wave functions should have a completely different form at large β, but coming up with the right trial wave function for which the relevant integrals can be done is clearly a nontrivial task as evidenced by the fact that some degree of flexibility was built into the trial wave function (4).

For bistable light bullets in 3D governed by W-shaped energy curves (basically two U's back to back) the situation gets even worse. As a simple example, $f(I)=a_1I-a_2I^2+a_3I^3-a_4I^4$ with $a_1,\ldots,a_4>0$ should yield a W-shaped energy curve on suitably adjusting the coefficients. Using Eq. (4) with $m=n=1$, we obtain (again using Table I) for the phase shift and energy, respectively,

$$\bar{\beta}\equiv\left[\frac{a_3}{a_1a_2}\right]\delta=\left[\frac{1}{6}-\frac{1}{\pi^2}\right]\bar{x}^2-\left[\frac{3I_{2,8}}{2\pi^2}\right]\bar{x}^6/\bar{R}+\left[\frac{12I_{2,10}}{5\pi^2}\right]\left[\frac{\bar{R}'}{\bar{R}}\right]\bar{x}^8, \tag{52}$$

with $\bar{R}\equiv a_1a_3/a_2^2$, $\bar{R}'\equiv a_2a_4/a_3^2$, and $\bar{x}^2\equiv(a_3/a_2)A_0^2$,

$$\bar{P}\equiv a_1^{3/2}(a_2/a_3)^{1/4}P=\frac{(\pi^2/12)\{[(\pi^2/18)+(2/3)]/((\pi^2/6)-1)\}^{3/2}}{\bar{x}\{1-[4I_{2,6}/(\pi^2/6-1)]\bar{x}^2/\bar{R}+[3I_{2,8}/(\pi^2/9-2/3)]\bar{x}^4/\bar{R}-[8I_{2,10}/5(\pi^2/18-1/3)](\bar{R}'/\bar{R})\bar{x}^6\}^{3/2}}. \tag{53}$$

For $\bar{R}=0.3$, $\bar{R}'=0.2$, $\bar{P}$ is a W-shaped function of $\bar{x}$ (i.e., amplitude) as shown in Fig. 8. However, as seen in Fig. 9, over the same range of $\bar{x}$, $\bar{\beta}$ not only turns over prematurely but *goes negative* before once again increasing. This leads to bizarre behavior of $\bar{P}_{\rm var}(\bar{\beta}_{\rm var})$ in the middle of the $\bar{\beta}_{\rm var}$ range.

Similarly, it is easy to show numerically that for, e.g., the saturable model

$$f(I)=\frac{I}{(1+aI)}-\frac{I}{(1+bI)}+\frac{eI}{(1+cI)},$$

a W-shaped energy curve occurs (not shown here) in 3D for a suitable choice of the parameters, e.g., $a=0.01$, $b=0.0101$, $c=2$, and $e=0.2$. Since it was unable to even reproduce the positive-slope leg of the U-shaped energy curve in 2D or 3D for the earlier saturable model, the trial wave function (4) is unable to reproduce the W-shaped energy in 3D for the above saturable model.

To apply the variational method to 3D and the bistable light-bullet problem in particular is going to involve a search for more suitable trial wave functions. Correctly calculating the phase shift for polynomial models appears to be much more of a difficulty than calculating the energy as a function of amplitude. Since for any saturable model $F(I)$ will involve logarithmic functions, the choice of possible trial wave functions for which subsequent integrals in the variational treatment can be done analytically is even more limited.

V. CONCLUSION

The variational approach has been applied to a study of bistable solitary waves of the first kind (BISOL1) in d dimensions for two representative models. For our choice of trial wave functions, the method works extremely well in one dimension but becomes less successful as d is increased. As discussed, this has practical implications as to the successful variational treatment of the bistable light-bullet problem.

[1] A. E. Kaplan, Phys. Rev. Lett. **55**, 1291 (1985); IEEE J. Quantum Electron. **QE-21**, 1538 (1985).

[2] R. H. Enns, S. S. Rangnekar, and A. E. Kaplan, Phys. Rev. A **35**, 466 (1987); **36**, 1270 (1987).

[3] R. H. Enns and S. S. Rangnekar, Phys. Rev. A **45**, 3354 (1992).

[4] D. E. Edmundson and R. H. Enns, Opt. Lett. **17**, 586 (1992).

[5] R. H. Enns, D. E. Edmundson, S. S. Rangnekar, and A. E. Kaplan, Opt. Quantum Electron. **24**, S1295 (1992).
[6] S. Gatz and J. Herrmann, IEEE J. Quantum Electron. **28**, 1732 (1992).
[7] J. Herrmann, Opt. Commun. **87**, 161 (1992).
[8] S. Eix and R. H. Enns, Phys. Rev. A **47**, 5009 (1993).
[9] R. H. Enns and D. E. Edmundson, Phys. Rev. A **47**, 4524 (1993).
[10] M. Desaix, D. Anderson, and M. Lisak, J. Opt. Soc. Am. B **8**, 2082 (1991).
[11] D. Anderson, Phys. Rev. A **27**, 3135 (1983).